VSP

Advanced Robotics 24 (2010) 1345–1364

ADVANCED ROBOTICS
brill.nl/ar

Full paper

A Riemannian-Geometric Approach for Intelligent Control and Fingertip Design of Multi-fingered Hands

Suguru Arimoto [a,b,*], **Morio Yoshida** [b], **Masahiro Sekimoto** [a] **and Ji-Hun Bae** [c]

[a] Research Organization of Science and Engineering, Ritsumeikan University, 1-1-1 Nojihigashi, Kusatsu, Shiga 525-8577, Japan

[b] RIKEN-TRI Collaboration Center, RIKEN, Nagoya, Aichi 463-0003, Japan

[c] Center for Cognitive Robotics Research, KIST, Seoul, South Korea

Received 7 August 2009; accepted 13 October 2009

Abstract

Based upon the analysis of modeling and control of two-dimensional (2-D) grasping and manipulation of arbitrary rigid objects under rolling contact constraints, geometrical conditions for the design of desired fingertip shapes of robot fingers are discussed from the Riemannian-geometric standpoint. A required condition is given as an inequality expressed in terms of quantities of the second fundamental form of fingertip contour curves, although the quantities do not enter into the Euler–Lagrange equation of motion of the overall fingers/object system. Satisfaction of the inequality is necessary for stabilization of grasping by using fingers–thumb opposable control signals without use of external sensings or knowledge of an object to be grasped. At the same time, asymptotic convergence of a solution to the closed-loop dynamics of 2-D precision prehension by a pair of multi-joint robot fingers is proved under rolling contact constraints and the existence of redundancy in the system's degrees of freedom. This is regarded as an extension of the Dirichlet–Lagrange stability theorem to a dynamical system with redundancy and geometric constraints.

Keywords

Multi-fingered hands, Riemannian geometry, fingers–thumb opposability, precision prehension, stable grasping

1. Introduction

In Napier's famous book [1], entitled *Hands*, he said that 'opposition of the thumb is one of the hallmarks by which humans can be authenticated as it were'. As to the fingers–thumb opposability, Napier also defined: 'Opposition is a movement

* To whom correspondence should be addressed. E-mail: arimoto@fc.ritsumei.ac.jp

 DOI:10.1163/016918610X501462

by which the pulp surface of the thumb is placed squarely in contact with — or diametrically opposite to — the terminal pads of one or all of the remaining digits'.

This paper tackles not only a control problem for stabilization of motion of precision prehension (two-dimensional (2-D) object grasping) based on the fingers–thumb opposability, but also a design problem of fingertip shapes that must be fit to the most important function of hands, i.e., fingers–thumb opposition. When fingertips are a rigid body, different from the softness of human digits, mathematical modeling of 2-D grasping becomes relatively easier even if rolling contact constraints are taken into account [2, 3]. However, if grasping of a 2-D object with arbitrary smooth contour curves is to be treated, modeling of rolling contact constraints becomes difficult because the constraints are regarded originally to be non-holonomic, as discussed in a representative text book [4]. In a typical 'ball–plate' problem of grasping when fingertips are hemispheric and an object to be grasped is a parallelepiped, it has been shown that the Pfaffian form expressing a rolling contact constraint is integrable and its integral is described in an explicit form. Very recently, in 2009, it was shown that Pfaffian forms of rolling contact constraints are integrable in the sense of Frobenius for a general class of 2-D graspings even if both the fingertips and object have arbitrary shapes [5]. In Ref. [5], the Euler–Lagrange equation of motion of the fingers/object system is derived, which are characterized by arclength parameters of contour curves along which rolling contact motions arise. At the same time, an update law of arclength parameters is derived as a first-order differential equation in which quantities of the second fundamental form of contour curves are involved. This follows from a differential-geometric assumption on rolling contact proposed by Nomizu [6].

This paper first summarizes the previous results of 2-D grasping under the circumstances of the arbitrary geometry of fingertip and object shapes, and shows that, in a special case when the object is a parallelopiped, stable grasping is realized by a control signal based upon the fingers–thumb opposability. It is then shown that the control signal can be regarded as a gradient of a potential function whose minimum is attained at an equilibrium posture. Then, necessary conditions for an adequate shape of fingertip contours are given by characterizing a relation of the curvatures of contour curves with changeable lengths between the contact point and the fingertip center. Compared with typical fingertips like a hemisphere, a type of the moon 13 days old, a cresent moon or an ellipse, a contour curve of the human thumb is mostly fit to minimization of the artificial potential function based on the fingers–thumb opposability. In Section 5, the necessity condition is enlarged by treating the arbitrary geometry of rigid objects based upon a testbed problem of stabilization of rotational motion by using a single robot finger. In the final section, a proof of convergence of motions of the closed-loop dynamics to an equilibrium posture of stable grasping is given in the case that the object is a parallelopiped. A general problem of finding a stable control signal for a class of 2-D objects with an arbitrary shape is still open and remains unsolved.

In Napier's book [1], John Hunter's principle is quoted at p. 9: 'structure was the intimate expression of function' and 'function was conditioned by environment'. By invoking three heros (Hunter, Charles Bell and Charles Darwin), Napier continued: 'John Hunter turned our attention from the structure of the hand to its function; Bell related the function of the hand to the environment; and Darwin demonstrated that the environment, by process of natural selection, gave birth to structure'.

2. Euler–Lagrange Equations of Motion

Very recently, a complete model of 2-D grasping of a rigid object with an arbitrary shape by a pair of robot fingers with arbitrarily given fingertip shapes (see Fig. 1) was presented based upon the differential-geometric assumptions of rolling contacts [2]. The assumptions are summarized as:

(i) Two contact points on the contour curves must coincide at a single common point without mutual penetration.

(ii) The two contours must have the same tangent at the common contact point.

As pointed out in previous papers [5, 7], these two conditions as a whole are equivalent to Nomizu's relation [6] concerning tangent vectors at the contact point and normals to the common tangent. As a result, a set of Euler–Lagrange equations of motion of the overall fingers/object system is presented in the following forms:

$$M\ddot{\mathbf{x}} - \sum_{i=1,2} (f_i \bar{\mathbf{n}}_{0i} + \lambda_i \bar{\mathbf{b}}_{0i}) = 0 \tag{1}$$

$$I\ddot{\theta} + \sum_{i=1,2} (-1)^i \{ f_i (\mathbf{b}_{0i}^{\mathrm{T}} \gamma_{0i}) - \lambda_i (\mathbf{n}_{0i}^{\mathrm{T}} \gamma_{0i}) \} = 0 \tag{2}$$

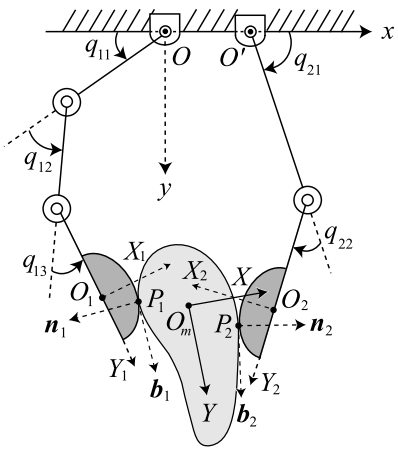

Figure 1. Pair of 2-D robot fingers with a curved fingertip makes rolling contact with a rigid object with a curved contour.

$$G_i(q_i)\ddot{q}_i + \left\{\frac{1}{2}\dot{G}_i(q_i) + S_i(q_i, \dot{q}_i)\right\}\dot{q}_i + f_i\{J_i^{\mathrm{T}}(q_i)\bar{\mathbf{n}}_{0i} - (-1)^i(\mathbf{b}_i^{\mathrm{T}}\gamma_i)\mathbf{e}_i\}$$
$$+ \lambda_i\{J_i^{\mathrm{T}}(q_i)\bar{\mathbf{b}}_{0i} - (-1)^i(\mathbf{n}_i^{\mathrm{T}}\gamma_i)\mathbf{e}_i\} = u_i, \quad i = 1, 2, \tag{3}$$

where q_i denotes the joint vector as $q_1 = (q_{11}, q_{12}, q_{13})^{\mathrm{T}}$ and $q_2 = (q_{21}, q_{22})^{\mathrm{T}}$, $\dot{\theta}$ denotes the angular velocity of rotation of the object around the object mass center O_m expressed by position vector $\mathbf{x} = (x, y)^{\mathrm{T}}$ in terms of the inertial frame coordinates O-xy and $J_i(q_i) = \partial\mathbf{r}_i/\partial q_i^{\mathrm{T}}$ for $i = 1, 2$, where $\mathbf{r}_i$ denotes the position of O_i in O-xy coordinates. It is implicitly assumed that all axes of rotation of finger joints are in the z-axis orthogonal to the horizontal xy-plane and, therefore, the effect of gravity is ignored. In general, there is no reason to equip each robot finger with three joints but the two joints must be necessary for further realization of dexterity like control of the orientation angle of an object if the object geometry is known. Equation (1) expresses the translational motion of the object with mass M and (2) its rotational motion with inertia moment I around the mass center O_m. At the contact point P_i, $\mathbf{b}_i$ denotes the unit tangent vector expressed in local coordinates of O_i-X_iY_i fixed to the fingertip of finger i ($i = 1, 2$) as shown in Figs 1 and 2, and $\mathbf{n}_i$ denotes the unit normal to the tangent expressed in terms of O_i-X_iY_i. Similarly, $\mathbf{b}_{0i}$ and $\mathbf{n}_{0i}$ are the unit tangent and normal at P_i expressed in terms of local coordinates O_m-XY fixed to the object as shown in Figs 1 and 2. All these unit vectors are determined uniquely from the assumptions (i) and (ii) on the rolling contact constraints at each contact point P_i dependently on each corresponding value s_i of arclength parameter for $i = 1, 2$ as shown in Fig. 2. In accordance with the assumptions (i) and (ii), a single length parameter s_1 is used commonly for expressing the position of contact point P_1 along the left fingertip contour and that of P_1 along the object contour at the left side. Similarly, s_2 is commonly used for expressing the location of contact point P_2 along $\mathbf{b}_{02}$ and $\mathbf{b}_2$. Equation (3) expresses joint motions of finger i with the inertia matrix $G_i(q_i)$ for $i = 1, 2$ and $\mathbf{e}_1 = (1, 1, 1)^{\mathrm{T}}$ and $\mathbf{e}_2 = (1, 1)^{\mathrm{T}}$. All position vectors γ_i and γ_{0i} for $i = 1, 2$ are defined in Fig. 2, and expressed in their

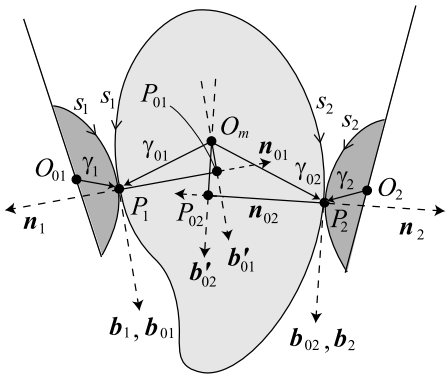

Figure 2. Definitions of tangent vectors $\mathbf{b}_i$ and $\mathbf{b}_{0i}$ and normals $\mathbf{n}_i$ and $\mathbf{n}_{0i}$ at contact points P_i for $i = 1, 2$.

corresponding local coordinates, respectively. Both the unit vectors $\bar{\mathbf{b}}_{0i}$ and $\bar{\mathbf{n}}_{0i}$ are expressed in the inertial frame coordinates as:

$$\bar{\mathbf{b}}_{0i} = \Pi_0 \mathbf{b}_{0i}, \qquad \bar{\mathbf{n}}_{0i} = \Pi_0 \mathbf{n}_{0i}, \quad \Pi_0 = (\mathbf{r}_X, \mathbf{r}_Y), \tag{4}$$

where $\Pi_0 \in SO(2)$, and $\mathbf{r}_X$ and $\mathbf{r}_Y$ denote the unit vectors of X- and Y-axes of the object in terms of the frame coordinates O-xy. In (1)–(3), f_i and λ_i are Lagrange multipliers that correspond to the following rolling contact constraints, respectively:

$$\begin{cases} Q_{bi} = (\mathbf{r}_i - \mathbf{r}_m)^{\mathrm{T}} \bar{\mathbf{b}}_{0i} + \mathbf{b}_i^{\mathrm{T}} \gamma_i - \mathbf{b}_{0i}^{\mathrm{T}} \gamma_{0i} = 0, \quad i = 1, 2 & (5) \\ Q_{ni} = (\mathbf{r}_i - \mathbf{r}_m)^{\mathrm{T}} \bar{\mathbf{n}}_{0i} - \mathbf{n}_i^{\mathrm{T}} \gamma_i - \mathbf{n}_{0i}^{\mathrm{T}} \gamma_{0i} = 0, \quad i = 1, 2, & (6) \end{cases}$$

where $\mathbf{r}_i$ denotes the position vector of the fingertip center O_i expressed in terms of the frame coordinates O-xy and $\mathbf{r}_m$ the position vector of O_m in terms of O-xy. In parallel with Euler–Lagrange equations (1)–(3), arclength parameters s_i $(i = 1, 2)$ should be governed by the following formulae of the first-order differential equation [5]:

$$\{\kappa_{0i}(s_i) + \kappa_i(s_i)\} \frac{\mathrm{d}s_i}{\mathrm{d}t} = (-1)^i (\dot{\theta} - \dot{p}_i), \quad i = 1, 2, \tag{7}$$

where $\kappa_i(s_i)$ denotes the curvature of the fingertip contour for $i = 1, 2$, $\kappa_{0i}(s_i)$ the curvature of the object contour at contact point P_i corresponding to length parameter s_i for $i = 1, 2$, $p_1 = q_{11} + q_{12} + q_{13}$, and $p_2 = q_{21} + q_{22}$. Throughout the paper we use $(\dot{})$ to denote the differentiation of the content of the parentheses ( ) in time t as $\dot{\theta} = \mathrm{d}\theta/\mathrm{d}t$ in (7) and $(')$ for that of ( ) in length parameter s_i as illustrated by $\gamma_i'(s_i) = \mathrm{d}\gamma_i(s_i)/\mathrm{d}s_i$. As discussed in the previous papers, we have:

$$\mathbf{b}_i(s_i) = \gamma_i'(s_i) \quad \left(= \frac{\mathrm{d}\gamma_i(s_i)}{\mathrm{d}s_i}\right), \qquad \mathbf{b}_{0i}(s_i) = \gamma_{0i}'(s_i), \quad i = 1, 2, \tag{8}$$

and:

$$\mathbf{n}_i(s_i) = \kappa_i(s_i) \mathbf{b}_i'(s_i), \qquad \mathbf{n}_{0i}(s_i) = \kappa_{0i}(s_i) \mathbf{b}_{0i}'(s_i), \quad i = 1, 2, \tag{9}$$

and further:

$$\mathbf{b}_i(s_i) = -\kappa_i(s_i) \mathbf{n}_i'(s_i), \qquad \mathbf{b}_{0i}(s_i) = -\kappa_{0i}(s_i) \mathbf{n}_{0i}'(s_i), \quad i = 1, 2. \tag{10}$$

It is well known from text books on differential geometry of curves and surfaces (see, e.g., Ref. [5]) that (9) and (10) constitute Frenet–Serre's formulae for the fingertip contour curves and object contours. Note that all equations (1)–(3) are characterized by length parameters s_i for $i = 1, 2$ through unit vectors $\mathbf{n}_{0i}$, $\mathbf{b}_{0i}$, $\mathbf{b}_i$, and $\mathbf{n}_i$, and vectors γ_{0i} and γ_i expressed in each local coordinates, but quantities of the second fundamental form of contour curves, i.e., $\kappa_i(s_i)$ and $\kappa_0(s_i)$ for $i = 1, 2$, do not enter into (1)–(3). It is shown that the set of Euler–Lagrange equations of motion from (1) to (3) can be derived by applying the variational principle to the Lagrangian of the system

$$L(X; s_1, s_2) = K(X, \dot{X}) - \sum_{i=1,2} (f_i Q_{ni} + \lambda_i Q_{bi}), \tag{11}$$

where X denotes the position state vector defined as:

$$X = (x, y, \theta, q_1^{\mathrm{T}}, q_2^{\mathrm{T}})^{\mathrm{T}}, \tag{12}$$

and:

$$K(X, \dot{X}) = \frac{M}{2}(\dot{x}^2 + \dot{y}^2) + \frac{I}{2}\dot{\theta}^2 + \sum_{i=1,2} \frac{1}{2}\dot{q}_i^{\mathrm{T}} G_i(q_i)\dot{q}_i. \tag{13}$$

Note that $K(X, \dot{X})$ is independent of the shape parameters s_1 and s_2, but Q_{ni} and Q_{bi} defined by (5) and (6) are dependent on s_i for $i = 1, 2$, respectively. The variational principle is written in the following form:

$$\int_{t_0}^{t_1} \{\delta L + u_1^{\mathrm{T}}\delta q_1 + u_2^{\mathrm{T}}\delta q_2\}\,\mathrm{d}t = 0. \tag{14}$$

From this it follows that:

$$G(X)\ddot{X} + \left(\frac{1}{2}\dot{G}(X) + S(X, \dot{X})\right)\dot{X} + \sum_{i=1,2}\left(f_i \frac{\partial}{\partial X} Q_{ni} + \lambda_i \frac{\partial}{\partial X} Q_{bi}\right)$$
$$= B\begin{pmatrix} u_1 \\ u_2 \end{pmatrix}, \tag{15}$$

where $G(X) = \mathrm{diag}(M, M, I, G_1(q_1), G_2(q_2))$, $S(X, \dot{X})$ is a skew-symmetric matrix and B denotes the 8×5 constant matrix defined as $B^{\mathrm{T}} = (0_{3\times5}, I_5)$, where $0_{3\times5}$ signifies the 3×5 zero matrix, and I_5 the 5×5 identity matrix.

3. Fingers–Thumb Opposable Control Signals

In order to design adequate control signals for a pair of multi-joint fingers as shown in Fig. 1, we suppose that the kinematics of both the robot fingers are known, and measurement data of joint angles and angular velocities are available in real-time, but the geometry of an object to be grasped is unknown and the location of its mass center together with its inclination angle cannot be measured or sensed. This supposition is reasonable because the structure of robot fingers is fixed for any object, but the object to be grasped is changeable from time to time. This standpoint is coincident to the start point of Riemannian geometry that, if the robot (both the robot fingers) has its own internal world, then the robot kinematics based upon quantities of the first fundamental form like $\gamma_i(s_i)$ and $\mathbf{b}_i(s_i)$ together with q_i and $\dot{q}_i$ must be accessible because these data are intrinsic to the robot's internal world. However, any quantities of the second fundamental form like $\kappa_i(s_i)$ $(i = 1, 2)$ cannot be determined from the robot's intrinsic world. By the same season, we assume that the positions of finger centers O_1 and O_2 denoted by $\mathbf{r}_1$ and $\mathbf{r}_2$ are accessible from the intrinsic robot world, and further the Jacobian matrices defined by $J_i(q_i) = \partial\mathbf{r}_i/\partial q_i^{\mathrm{T}}$ for $i = 1, 2$ are also assumed to be intrinsic, i.e., real-time computable. Thus, let us now consider a class of control signals defined by the form:

$$u_i = -c_i\dot{q}_i + (-1)^i \beta J_i^{\mathrm{T}}(q_i)(\mathbf{r}_1 - \mathbf{r}_2) - \alpha_i \hat{N}_i \mathbf{e}_i, \quad i = 1, 2, \tag{16}$$

where β stands for a position feedback gain common for $i = 1, 2$ with physical unit N/m, α is also a positive constant common for $i = 1, 2$, $\hat{N}_i$ is defined as:

$$\hat{N}_i = \mathbf{e}_i^{\mathrm{T}}\{q_i(t) - q_i(0)\} = p_i(t) - p_i(0), \quad i = 1, 2, \tag{17}$$

and c_i denotes a positive constant for joint damping for $i = 1, 2$. The first term on the right-hand side of (16) stands for damping shaping, the second term plays a role of fingers–thumb opposition and the last term avoids possibly some excess motion of rotation of the object through contacts. Note that the sum of inner products of u_i and $\dot{q}_i$ for $i = 1, 2$ is given by:

$$\sum_{i=1,2} \dot{q}_i^{\mathrm{T}} u_i = -\frac{\mathrm{d}}{\mathrm{d}t}\left\{\frac{\beta}{2}\|\mathbf{r}_1 - \mathbf{r}_2\|^2 + \sum_{i=1,2}\frac{\alpha_i}{2}\hat{N}_i^2\right\} - \sum_{i=1,2} c_i\|\dot{q}_i\|^2. \tag{18}$$

Substitution of control signals of (16) into (3) yields:

$$\begin{aligned} G_i\ddot{q}_i + \left\{\frac{1}{2}\dot{G}_i + S_i\right\}\dot{q}_i + c_i\dot{q}_i - (-1)^i\beta J_i^{\mathrm{T}}(\mathbf{r}_1 - \mathbf{r}_2) + \alpha_i\hat{N}_i\mathbf{e}_i \\ + f_i\{J_i^{\mathrm{T}}\bar{\mathbf{n}}_{0i} - (-1)^i(\mathbf{b}_i^{\mathrm{T}}\gamma_i)\mathbf{e}_i\} \\ + \lambda_i\{J_i^{\mathrm{T}}\bar{\mathbf{b}}_{0i} - (-1)^i(\mathbf{n}_i^{\mathrm{T}}\gamma_i)\mathbf{e}_i\} = 0, \quad i = 1, 2. \end{aligned} \tag{19}$$

Hence, the overall closed-loop dynamics is composed of the set of Euler–Lagrange equations of (1), (2) and (19) that are subject to four algebraic constraints of (5) and (6), and the pair of the first-order differential equations of (7) that governs the update law of arclength parameters s_1 and s_2. It should be also remarked that, according to (18), the sum of inner products of (1) and $\dot{\mathbf{x}}$, (2) and $\dot{\theta}$, and (19) and $\dot{q}_i$ for $i = 1, 2$ yields the energy relation:

$$\frac{\mathrm{d}}{\mathrm{d}t}E(X, \dot{X}) = -\sum_{i=1,2} c_i\|\dot{q}_i\|^2, \tag{20}$$

where:

$$E(X, \dot{X}) = K(X, \dot{X}) + P(X) \tag{21}$$

$$P(X) = \frac{\beta}{2}\|\mathbf{r}_1 - \mathbf{r}_2\|^2 + \sum_{i=1,2}\frac{\alpha_i}{2}\hat{N}_i^2, \tag{22}$$

and $K(X, \dot{X})$ is the total kinetic energy defined by (13), and $P(X)$ is called the artificial potential energy that is a scalar function depending on only q_1 and q_2. It is important to note that the closed-loop dynamics of (1), (2) and (19) can be written into the general form, correspondingly to (15):

$$\begin{aligned} G(X)\ddot{X} + \left\{\frac{1}{2}\dot{G}(X) + S(X, \dot{X}) + C\right\}\dot{X} + \frac{\partial P(X)}{\partial X} \\ + \sum_{i=1,2}\left(f_i\frac{\partial}{\partial X}Q_{ni} + \lambda_i\frac{\partial}{\partial X}Q_{bi}\right) = 0, \end{aligned} \tag{23}$$

where $C = \mathrm{diag}(0_2, 0, c_1 I_3, c_2 I_2)$. This can be also obtained by applying the principle of variation to the Lagrangian:

$$L = K(X, \dot{X}) - P(X) - \sum_{i=1,2} (f_i Q_{ni} + \lambda_i Q_{bi}). \tag{24}$$

4. Necessary Conditions for the Design of Fingertip Shape

It is known [8] that, in a simple case of 'ball–plate' pinching, a solution to the closed-loop dynamics corresponding to (23) under some holonomic constraints of rolling contacts converges to a steady (equilibrium) state that minimizes the potential $P(X)$ under the constraints. However, a stabilization problem of control signals like (16) still remains unsolved or rather has not yet been tackled not only in a general setup of arbitrary geometry like the situation shown in Fig. 1, but also in a more simple case where the object to be grasped is a parallelepiped but the fingertip shapes are arbitrary. In this paper, we will tackle this simple problem and show that minimization of such an artifically introduced potential can lead to stable grasping under some good design of fingertip shapes (Fig. 3).

First, we remark that, since the first term of $P(X)$ in (22) is the squared norm of the vector $\overrightarrow{O_2 O_1}$ times $\beta/2$, it must be a function only dependent on length parameters s_1 and s_2. Then, it will be that minimization of the squared norm $\|\mathbf{r}_1 - \mathbf{r}_2\|^2$ over rolling contact motions is attained when the straight line $\overline{P_1 P_2}$ connecting the two contact points becomes parallel to the vector $(\mathbf{r}_1 - \mathbf{r}_2)$. That is, $U(X)$ $(=(\beta/2)\|\mathbf{r}_1 - \mathbf{r}_2\|^2)$ is minimized when $\overline{O_1 O_2}$ becomes parallel to $\overline{P_1 P_2}$. To show this directly from the set of Euler–Lagrange equations (1), (2) and (19) seems difficult even in this case. Instead, we remark that $(\mathbf{r}_1 - \mathbf{r}_2)$ can be expressed in terms of length parameters s_i for $i = 1, 2$ as:

$$\mathbf{r}_1 - \mathbf{r}_2 = -\Pi_1 \gamma_1 + \Pi_2 \gamma_2 + \Pi_0(\gamma_{01} - \gamma_{02}), \tag{25}$$

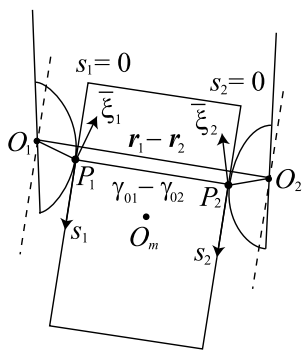

Figure 3. Minimization of the squared norm $\|\mathbf{r}_1 - \mathbf{r}_2\|^2$ over rolling motions is attained when the straight line $\overline{P_1 P_2}$ connecting the two contact points becomes parallel to the vector $(\mathbf{r}_1 - \mathbf{r}_2)$, i.e., $\overline{O_1 O_2}$ becomes parallel to $\overline{P_1 P_2}$.

where $\Pi_i \in SO(2)$ denotes the rotational matrix of O_i-X_iY_i to be expressed in the frame coordinates O-xy. Since the object is rectangular, all $\mathbf{b}_{0i}$ and $\mathbf{n}_{0i}$ for $i = 1, 2$ are invariant under the change of s_i for $i = 1, 2$. Therefore, as seen from Fig. 3, if the object width is denoted by $l_{\rm w}$ and zero points of s_1 and s_2 are set as shown in Fig. 3, then it is possible to write (25) as:

$$\mathbf{r}_1 - \mathbf{r}_2 = (s_1 - s_2)\bar{\mathbf{b}}_{01} + (-\mathbf{b}_1^{\rm T}\gamma_1 + \mathbf{b}_2^{\rm T}\gamma_2)\bar{\mathbf{b}}_{01} - l_{\rm w}\bar{\mathbf{n}}_{01} + (\mathbf{n}_1^{\rm T}\gamma_1 + \mathbf{n}_2^{\rm T}\gamma_2)\bar{\mathbf{n}}_{01}. \quad (26)$$

Since $\bar{\mathbf{b}}_{01} \perp \bar{\mathbf{n}}_{01}$, $U(X)$ can be expressed as:

$$\begin{aligned} U(X) &= \frac{\beta}{2}\|\mathbf{r}_1 - \mathbf{r}_2\|^2 = \frac{\beta}{2}\{d^2(s_1, s_2) + l^2(s_1, s_2)\} \\ &= U(s_1, s_2), \end{aligned} \quad (27)$$

where:

$$d(s_1, s_2) = s_1 - s_2 - \mathbf{b}_1^{\rm T}\gamma_1 + \mathbf{b}_2^{\rm T}\gamma_2 \quad (28)$$

$$l(s_1, s_2) = -l_w + (\mathbf{n}_1^{\rm T}\gamma_1 + \mathbf{n}_2^{\rm T}\gamma_2). \quad (29)$$

Note that the artificial potential $U(X)$ can be regarded as a scalar function defined in terms of length parameters s_1 and s_2. When minimization of $U(s_1, s_2)$ over some parameter intervals $s_i \in I_i = (a_i, b_i)$ is considered for $i = 1, 2$, it is important to note that the vector $(\mathbf{r}_1 - \mathbf{r}_2)$ is originally subject to the constraint:

$$V(s_1, s_2) = (\mathbf{r}_1 - \mathbf{r}_2)^{\rm T}\bar{\mathbf{n}}_{01} - \mathbf{n}_1^{\rm T}\gamma_1 - \mathbf{n}_2^{\rm T}\gamma_2 - \mathbf{n}_{01}^{\rm T}\gamma_{01} - \mathbf{n}_{02}^{\rm T}\gamma_{02} = 0, \quad (30)$$

which is obtained by subtraction of Q_{n2} from Q_{n1} defined in (5) and (6). Hence, by introducing a Lagrange multiplier η, minimization of the function:

$$W(s_1, s_2; \eta) = U(s_1, s_2) + \eta V(s_1, s_2), \quad (31)$$

must be equivalent to that of $U(X)$. Then it follows that:

$$\frac{\partial W}{\partial s_i} = (-1)^i \beta\kappa_i(\mathbf{r}_1 - \mathbf{r}_2)^{\rm T}\bar{\boldsymbol{\xi}}_i + \eta\kappa_i\mathbf{b}_i^{\rm T}\gamma_i, \quad i = 1, 2, \quad (32)$$

where we define, for abbreviation:

$$\bar{\boldsymbol{\xi}}_i = (\mathbf{n}_i^{\rm T}\gamma_i)\bar{\mathbf{b}}_{0i} + (\mathbf{b}_i^{\rm T}\gamma_i)\bar{\mathbf{n}}_{0i}, \quad i = 1, 2. \quad (33)$$

The derivation of this equation is discussed in Appendix A. At this stage, we remark that the vectors $\bar{\boldsymbol{\xi}}_i$ for $i = 1, 2$ appear at contact points P_1 and P_2 as indicated in Fig. 3. Evidently from the right-hand side of (32), if we set:

$$\eta = \beta(\mathbf{r}_1 - \mathbf{r}_2)^{\rm T}\bar{\mathbf{n}}_{01} \quad (= -\beta(\mathbf{r}_1 - \mathbf{r}_2)^{\rm T}\bar{\mathbf{n}}_{02}), \quad (34)$$

and at the same time:

$$(\mathbf{r}_1 - \mathbf{r}_2)^{\rm T}\bar{\mathbf{b}}_{0i} = 0, \quad i = 1, 2, \quad (35)$$

then (32) implies:

$$\frac{\partial W}{\partial s_i} = 0, \quad i = 1, 2. \quad (36)$$

In view of the geometrical meaning of (35) that the vector $\overrightarrow{O_2O_1} \perp \bar{\mathbf{b}}_{0i}$, when $\mathbf{r}_1 - \mathbf{r}_2$ becomes perpendicular to $\mathbf{b}_{0i}$ from some starting posture by rolling contact motion, s_i for $i = 1, 2$ must have the same value s^* and $\mathbf{b}_1^{\mathrm{T}}\gamma_1 = \mathbf{b}_2^{\mathrm{T}}\gamma_2$. That is, satisfaction of the conditions:

$$s_1 = s_2 = s^*, \qquad \mathbf{b}_1^{\mathrm{T}}\gamma_1 = \mathbf{b}_2^{\mathrm{T}}\gamma_2, \tag{37}$$

reduces to that $\overrightarrow{O_2O_1}$ becomes parallel to $\overrightarrow{P_2P_1}$ as shown in Fig. 3. Under (37):

$$\left.\frac{\partial W}{\partial s_i}\right|_{s_i=s^*} = 0, \quad i = 1, 2. \tag{38}$$

Finally, it is important to check the positivity of the Hessian matrix $H = (\partial^2 U/\partial s_i\, \partial s_j)$. Bearing in mind the form of (32) together with (34), we obtain (see the details in Appendix A):

$$\begin{aligned}\left.\frac{\partial^2 U}{\partial s_i\, \partial s_i}\right|_{s_i=s^*} &= \kappa_i(-1)^i \beta(\mathbf{r}_1 - \mathbf{r}_2)^{\mathrm{T}}\bar{\mathbf{n}}_{0i}(\kappa_i \mathbf{n}_i^{\mathrm{T}}\gamma_i + \mathbf{b}_i^{\mathrm{T}}\gamma_i') \\ &= -\beta l(s_1, s_2)\kappa_i^2\left(\frac{1}{\kappa_i} + \mathbf{n}_i^{\mathrm{T}}\gamma_i\right), \quad i = 1, 2,\end{aligned} \tag{39}$$

and:

$$\left.\frac{\partial^2 U}{\partial s_1\, \partial s_2}\right|_{s_i=s^*} = 0, \tag{40}$$

where $l(s_1, s_2)$ is defined by (29). Since $l(s_1, s_2) < 0$ from the geometrical meaning of the situation shown in Fig. 3, it is possible to conclude that the potential function $U(s_1, s_2)$ is minimized at the posture satisfying (37) provided that:

$$\frac{1}{\kappa_i(s_i)} > -\mathbf{n}_i^{\mathrm{T}}(s_i)\gamma_i(s_i), \quad i = 1, 2, \tag{41}$$

for all s_i belonging to $(s^* - \delta_i, s^* + \delta_i)$ with some $\delta_i > 0$ for $i = 1, 2$.

Geometric and physical meanings of (41) are well illustrated in Fig. 4. Even if the fingertip is spherical and its curvature $\kappa(s)$ is constant (i.e., equal to $1/r$, where r denotes the radius), a design of fingertip shape like a moon 13 days old does not satisfy the inequality of (41), since the center of the sphere is located inside the fingertip (Fig. 4a). In the case of a fingertip like a crescent moon shown in Fig. 4b, however, the inequality of (41) is satisfied. It is interesting to note that, in the case of an elliptic fingertip, the inequality of (41) is satisfied in the vicinity of contact position P_1 as shown in Fig. 5a when the line $\overline{O_1P_1}$ is perpendicular to the Y_1-axis, but there arise possible contact points denoted by P' that may not satisfy (41), when P' moves further toward the endpoint P_0 along the contour of the ellipsoid (Fig. 5b).

A mathematical proof of a solution trajectory to the closed-loop dynamics of (1), (2) and (19) under holonomic constraints of (5) and (6) together with the set of first-order differential equations of (7) starting from a posture in a neighborhood the equilibrium state shown in Fig. 3 will be discussed in Section 6.

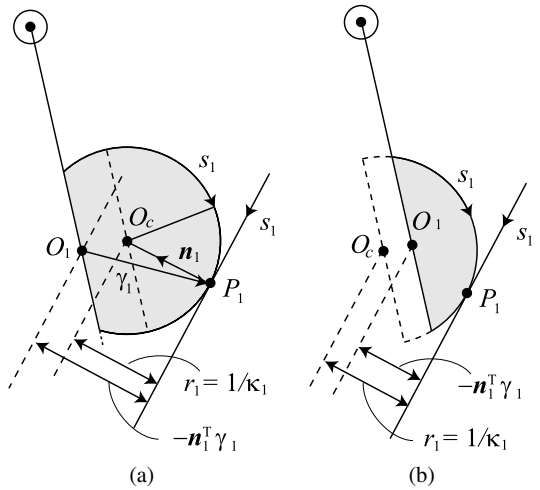

Figure 4. Design of a fingertip geometry is sensitive to the necessary condition for minimization of the artificial potential $U(s_1, s_2)$. (a) Fingertip like a moon 13 days old. (b) Fingertip like a crescent moon.

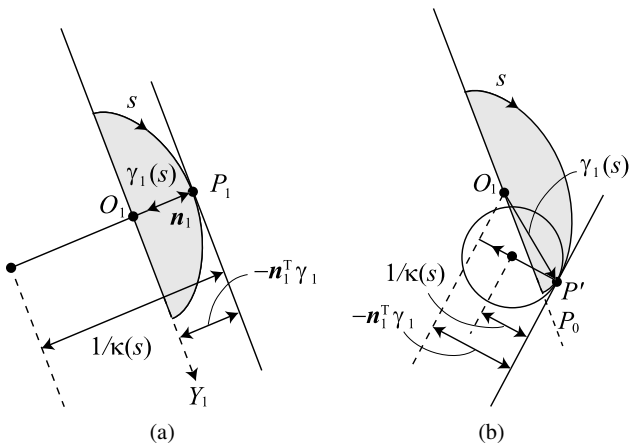

Figure 5. Fingertip design using a half of the ellipse. (a) Smallest curvature arises when $\overline{O_1P_1} \perp Y_1$-axis. (b) Curvature increases as P' runs along the contour toward the Y_1-axis.

5. Further Necessity of Fingertip Curvatures

In order to obtain a more robust condition on the design of the shape of a robot finger against more generality of the geometry of objects to be grasped stably, consider a testbed control problem of grasping a rigid object with an arbitrary geometry by a planar multi-joint robot finger as depicted in Fig. 6. In this problem, the object is pivoted around the point O_m fixed to the inertial frame O-xy. The object contour curve is denoted by $\gamma_0(s)$ with the aid of the arclength parameter expressed in local coordinates O_m-XY fixed to the object and the fingertip contour curve by $\gamma_1(s)$ expressed in local coordinates O_1-X_1Y_1 fixed to the fingertip as shown in Fig. 6.

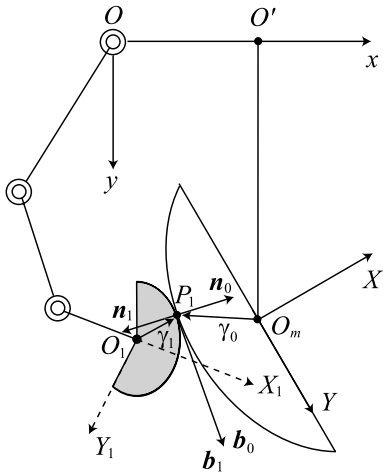

Figure 6. Testbed control problem of grasping a rigid object with arbitrary geometry.

Also, unit tangent vector $\mathbf{b}_1$ and normal $\mathbf{n}_1$ at contact point P_1 along the fingertip contour and similarly $\mathbf{b}_0$ and $\mathbf{n}_0$ at P_1 along the object contour are defined as shown in Fig. 6. It is shown in the previous paper [5] that the Euler–Lagrange equations of motion of this finger/object system are described in the forms:

$$I\ddot{\theta} - f(\gamma_0^{\mathrm{T}}\mathbf{b}_0) + \lambda(\gamma_0^{\mathrm{T}}\mathbf{n}_0) = 0 \tag{42}$$

$$G(q)\ddot{q} + \left\{\frac{1}{2}\dot{G}(q) + S(q,\dot{q})\right\}\dot{q} + f\{J_1^{\mathrm{T}}(q)\bar{\mathbf{n}}_0 + (\gamma_1^{\mathrm{T}}\mathbf{b}_1)\mathbf{e}\} + \lambda\{J_1^{\mathrm{T}}(q)\bar{\mathbf{b}}_0 + (\gamma_1^{\mathrm{T}}\mathbf{n}_1)\mathbf{e}\} = u, \tag{43}$$

where $\bar{\mathbf{n}}_0 = \Pi_0\mathbf{n}_0$, $\bar{\mathbf{b}}_0 = \Pi_0\mathbf{b}_0$, $\Pi_0 \in SO(2)$ with respect to the counterclockwise rotation angle θ from x-axis in the O-xy frame coordinates, I and $G(q)$ denote the object inertia moment around O_m and the finger inertia matrix, respectively, and $q = (q_{11}, q_{12}, q_{13})^{\mathrm{T}}$ and $\mathbf{e}_1 = (1,1,1)^{\mathrm{T}}$. If we use a control signal:

$$u = -c\dot{q} - \beta J_1^{\mathrm{T}}(q)(\mathbf{r}_1 - \mathbf{r}_0), \tag{44}$$

where $\mathbf{r}_1$ and $\mathbf{r}_0$ denote position vectors $\overrightarrow{OO_1}$ and $\overrightarrow{OO_m}$, respectively, and β and c are an appropriate positive constant, then the closed-loop dynamics obtained by substituting (44) into (43) can be written as:

$$G(q)\ddot{q} + \left\{\frac{1}{2}\dot{G} + S\right\}\dot{q} + c\dot{q} + \beta J_1^{\mathrm{T}}(q)(\mathbf{r}_1 - \mathbf{r}_0) + f\{J_1^{\mathrm{T}}(q)\bar{\mathbf{n}}_0 + (\gamma_1^{\mathrm{T}}\mathbf{b}_1)\mathbf{e}\} + \lambda\{J_1^{\mathrm{T}}(q)\bar{\mathbf{b}}_0 + (\gamma_1^{\mathrm{T}}\mathbf{n}_1)\mathbf{e}\} = 0. \tag{45}$$

Evidently the set of this equation and (42) can be regarded as the Euler–Lagrange equations of motion derived from applying the variational principle to the Lagrangian:

$$L = K(X,\dot{X}) - U(X) - fQ_n - \lambda Q_b, \tag{46}$$

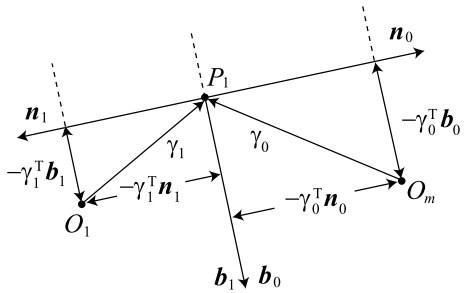

Figure 7. Geometric meaning of the length of $\overline{O_1 O_m}$.

where $X = (\theta, q^{\mathrm{T}})^{\mathrm{T}}$ and:

$$U(X) = \frac{\beta}{2}\|\mathbf{r}_1 - \mathbf{r}_0\|^2 \tag{47}$$

$$\begin{cases} Q_n = (\mathbf{r}_1 - \mathbf{r}_0)^{\mathrm{T}}\bar{\mathbf{n}}_0 - (\gamma_0^{\mathrm{T}}\mathbf{n}_0 + \gamma_1^{\mathrm{T}}\mathbf{n}_1) & (48) \\ Q_b = (\mathbf{r}_1 - \mathbf{r}_0)^{\mathrm{T}}\bar{\mathbf{b}}_0 - (\gamma_0^{\mathrm{T}}\mathbf{b}_0 - \gamma_1^{\mathrm{T}}\mathbf{b}_1). & (49) \end{cases}$$

It should be remarked that $Q_n = 0$ and $Q_b = 0$ as seen from the geometric meaning shown in Fig. 7. Note that $Q_b = 0$ plays a role of holonomic constraint of rolling contact in the tangent direction and $Q_n = 0$ that of contact in the normal direction. However, it is not obvious to see from the set of closed-loop dynamics of (42) and (45) what condition on the state of motion establishes stable grasping. To gain a physical and geometric insight into the problem, note that the vector $(\mathbf{r}_1 - \mathbf{r}_0)$ can be written in the form:

$$\mathbf{r}_1 - \mathbf{r}_0 = (\gamma_0^{\mathrm{T}}\mathbf{n}_0 + \gamma_1^{\mathrm{T}}\mathbf{n}_1)\bar{\mathbf{n}}_0 + (\gamma_0^{\mathrm{T}}\mathbf{b}_0 - \gamma_1^{\mathrm{T}}\mathbf{b}_1)\bar{\mathbf{b}}_0, \tag{50}$$

and the right-hand side depends on only θ in Π_0 and the length parameter s. Bearing this in mind, define:

$$\begin{cases} \Delta f = f + \beta(\gamma_0^{\mathrm{T}}\mathbf{n}_0 + \gamma_1^{\mathrm{T}}\mathbf{n}_1) \\ \Delta\lambda = \lambda + \beta(\gamma_0^{\mathrm{T}}\mathbf{b}_0 - \gamma_1^{\mathrm{T}}\mathbf{b}_1) \end{cases} \tag{51}$$

$$N_1 = (\gamma_1^{\mathrm{T}}\mathbf{b}_1)(-\gamma_0^{\mathrm{T}}\mathbf{n}_0) - (-\gamma_1^{\mathrm{T}}\mathbf{n}_1)(-\gamma_0^{\mathrm{T}}\mathbf{b}_0), \tag{52}$$

and see that (42) and (45) can be rewritten into the following formulae:

$$I\ddot{\theta} - \Delta f(\gamma_0^{\mathrm{T}}\mathbf{b}_0) + \Delta\lambda(\gamma_0^{\mathrm{T}}\mathbf{n}_0) - \beta N_1 = 0 \tag{53}$$

$$\begin{aligned} G(q)\ddot{q} + \left\{\frac{1}{2}\dot{G} + S\right\}\dot{q} + c\dot{q} + \Delta f\{J_1^{\mathrm{T}}\bar{\mathbf{n}}_0 + (\gamma_1^{\mathrm{T}}\mathbf{b}_1)\mathbf{e}\} \\ + \Delta\lambda\{J_1^{\mathrm{T}}\bar{\mathbf{b}}_0 + (\gamma_1^{\mathrm{T}}\mathbf{n}_1)\mathbf{e}\} + \beta N_1\mathbf{e} = 0. \end{aligned} \tag{54}$$

It should be remarked that both the (53) and (54) depend on length parameter s, but not on quantities of the second fundamental form of contour curves. Instead,

the length parameter s must be governed by the following first-order differential equation:

$$\{\kappa_1(s) + \kappa_0(s)\}\frac{\mathrm{d}s}{\mathrm{d}t} = \dot{q}^{\mathrm{T}}\mathbf{e} - \dot{\theta}, \tag{55}$$

where κ_1 denotes the curvature of the finger contour and κ_0 that of the object contour. Then, note that the artificial potential $U(X)$ can be regarded as a scalar function of the length parameter in a geometric meaning shown in Fig. 7 such that:

$$\begin{aligned} U(X) &= \frac{\beta}{2}\|\mathbf{r}_1 - \mathbf{r}_0\|^2 = \frac{\beta}{2}\{(\gamma_0^{\mathrm{T}}\mathbf{n}_0 + \gamma_1^{\mathrm{T}}\mathbf{n}_1)^2 + (\gamma_0^{\mathrm{T}}\mathbf{b}_0 - \gamma_1^{\mathrm{T}}\mathbf{b}_1)^2\} \\ &= U(s). \end{aligned} \tag{56}$$

Thus, it is possible to see that the set of (53) and (54) can be regarded as the Euler–Lagrange equation obtained by applying the principle of variation to the Lagrangian:

$$L(X, \dot{X}, s) = K(X, \dot{X}) - U(s) - \Delta f\, Q_n(X, s) - \Delta\lambda\, Q_b(X, s). \tag{57}$$

The details are given in Appendix B. To show under what condition the function $U(s)$ is minimized, it is necessary to take differentiation of $U(s)$ in s, that results in:

$$\begin{aligned} \beta^{-1}\frac{\mathrm{d}U}{\mathrm{d}s} &= (\gamma_0^{\mathrm{T}}\mathbf{n}_0 + \gamma_1^{\mathrm{T}}\mathbf{n}_1)(\mathbf{b}_0^{\mathrm{T}}\mathbf{n}_0 + \mathbf{b}_1^{\mathrm{T}}\mathbf{n}_1 - \kappa_0\gamma_0^{\mathrm{T}}\mathbf{b}_0 - \kappa_1\gamma_1^{\mathrm{T}}\mathbf{b}_1) \\ &\quad + (-\gamma_0^{\mathrm{T}}\mathbf{b}_0 + \gamma_1^{\mathrm{T}}\mathbf{b}_1)(-\mathbf{b}_0^{\mathrm{T}}\mathbf{b}_0 + \mathbf{b}_1^{\mathrm{T}}\mathbf{b}_1 - \kappa_0\gamma_0^{\mathrm{T}}\mathbf{n}_0 + \kappa_1\gamma_1^{\mathrm{T}}\mathbf{n}_1) \\ &= -(\kappa_0 + \kappa_1)\{(\gamma_1^{\mathrm{T}}\mathbf{n}_1)(\gamma_0^{\mathrm{T}}\mathbf{n}_0) + (\gamma_1^{\mathrm{T}}\mathbf{b}_1)(\gamma_0^{\mathrm{T}}\mathbf{n}_0)\}. \end{aligned} \tag{58}$$

From the geometric meaning shown in Fig. 8, this derivative vanishes if and only if the area A_0 equals to the area A_1, i.e.:

$$A_0 = (\gamma_1^{\mathrm{T}}\mathbf{b}_1)(-\gamma_0^{\mathrm{T}}\mathbf{n}_0) = (-\gamma_0^{\mathrm{T}}\mathbf{b}_0)(-\gamma_1^{\mathrm{T}}\mathbf{n}_1) = A_1. \tag{59}$$

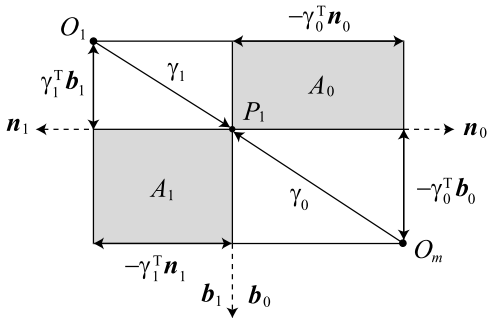

Figure 8. Minimization of $U(s)$ is attained if and only if the straight line O_1O_m meets the contact point P_1 or the area A_0 $(= -\gamma_0^{\mathrm{T}}\mathbf{n}_0 \times \gamma_1^{\mathrm{T}}\mathbf{b}_1)$ is equal to A_1 $(= \gamma_1^{\mathrm{T}}\mathbf{n}_1 \times \gamma_0\mathbf{b}_0)$.

Hence, it follows from (52) that:

$$\beta^{-1}\frac{\mathrm{d}U(s)}{\mathrm{d}s} = (\kappa_0+\kappa_1)N_1(s) = (\kappa_0+\kappa_1)(A_0 - A_1). \tag{60}$$

Next, to take the second derivative of $U(s)$ at $N_1 = 0$, we calculate the derivative N_1 in s in such a way that:

$$\begin{aligned}\frac{\partial N_1}{\partial s} &= (1+\kappa_1\gamma_1^{\mathrm{T}}\mathbf{n}_1)(-\gamma_0^{\mathrm{T}}\mathbf{n}_0) + (\gamma_1^{\mathrm{T}}\mathbf{b}_1)(-\mathbf{b}_0^{\mathrm{T}}\mathbf{n}_0 - \kappa_0\gamma_0^{\mathrm{T}}\mathbf{b}_0)\\ &\quad - (\mathbf{b}_1^{\mathrm{T}}\mathbf{n}_1 - \kappa_1\gamma_1^{\mathrm{T}}\mathbf{b}_1)(\gamma_0^{\mathrm{T}}\mathbf{b}_0) - (\gamma_1^{\mathrm{T}}\mathbf{n}_1)(1+\kappa_0\gamma_0^{\mathrm{T}}\mathbf{n}_0)\\ &= -(\gamma_0^{\mathrm{T}}\mathbf{n}_0 + \gamma_1^{\mathrm{T}}\mathbf{n}_1) + (\kappa_0+\kappa_1)\{(\gamma_0^{\mathrm{T}}\mathbf{b}_0)(\gamma_1^{\mathrm{T}}\mathbf{b}_1) - (\gamma_0^{\mathrm{T}}\mathbf{n}_0)(\gamma_1^{\mathrm{T}}\mathbf{n}_1)\}.\end{aligned} \tag{61}$$

For the sake of simplifying notations, define:

$$l_{ni} = -\gamma_i^{\mathrm{T}}\mathbf{n}_i, \qquad l_{bi} = \gamma_i^{\mathrm{T}}\mathbf{b}_i. \tag{62}$$

Then, from (60) and (61) it follows that:

$$\beta^{-1}\frac{\mathrm{d}^2U(s)}{\mathrm{d}s^2}\bigg|_{N_1=0} = (\kappa_0+\kappa_1)\{l_{n0} + l_{n1} + (\kappa_0+\kappa_1)(l_{b0}l_{b1} - l_{n0}l_{n1})\}. \tag{63}$$

Since $N_1 = 0$ means $l_{b1} = -(l_{b0}l_{n1})/l_{n0}$, the Hessian (the second derivative of $U(s)$) becomes positive when the following inequality is satisfied:

$$\kappa_0+\kappa_1 < \frac{l_{n0}+l_{n1}}{l_{n0}l_{n1} - l_{b0}l_{b1}} = \frac{(1/l_{n0}) + (1/l_{n1})}{1+\varepsilon_0}, \tag{64}$$

where ε_0 is defined as follows:

$$\varepsilon_0 = -l_{b0}l_{b1}/l_{n0}l_{n1} = l_{b0}^2/l_{n0}^2. \tag{65}$$

Thus, it is possible to conclude that, for any object with a smooth contour satisfying:

$$\frac{1}{\kappa_0} > (1+\varepsilon_0)l_{n0} = -(1+\varepsilon_0)\mathbf{n}_0^{\mathrm{T}}\gamma_0, \tag{66}$$

if the curvature of the fingertip satisfies:

$$\frac{1}{\kappa_1(s)} > (1+\varepsilon_0)l_{n1} = -(1+\varepsilon_0)\mathbf{n}_1^{\mathrm{T}}\gamma_1, \tag{67}$$

then the Hessian becomes positive and minimization of $U(s)$ is attained at $s = s^*$ such that $N_1(s^*) = 0$. Inequality (67) is a little more restrictive for $\kappa_1(s)$ than inequality (41).

Further comparison of (67) with (41) gives us an interesting observation that a typical human thumb has a contour curve shown in Fig. 9, which has a good margin ε_0 of (65) compared to other fingertip examples illustrated in Figs 4 and 5.

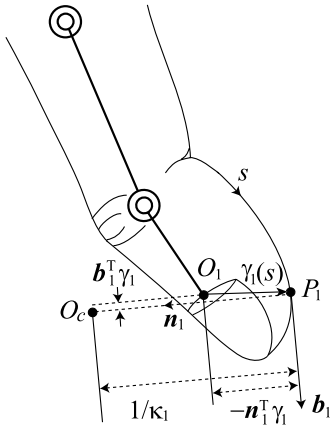

Figure 9. Sketch of a human-like thumb, where the fingertip center O_1 is located beneath the base of the fingernail.

6. Extension of the Dirichlet–Lagrange Theorem for Pinching a Rectangular Object

In this section, we show that, when the line connecting the contact points P_1 and P_2 becomes parallel to the line $\overline{O_1O_2}$ as shown in Fig. 3, $U(s_1, s_2)$ is minimized under the constraint of $V = 0$ [see (30)], and at the same time any solution to the set of closed-loop dynamics (1), (2) and (19) under rolling constraints (5) and (6) converges asymptotically to such an equilibrium posture, provided that the solution trajectory starts in a neighborhood of the equilibrium state. To do this, define:

$$\begin{cases} \Delta f_i = f_i + \beta l(s_1, s_2) & (68) \\ \Delta\lambda_i = \lambda_i - (-1)^i \beta d(s_1, s_2), & (69) \end{cases}$$

and note that:

$$-(-1)^i \beta J_i^{\mathrm{T}}(\mathbf{r}_1 - \mathbf{r}_2) = \beta J_i^{\mathrm{T}}\{l\bar{\mathbf{n}}_{0i} - (-1)^i d\bar{\mathbf{b}}_{0i}\}, \qquad i = 1, 2. \tag{70}$$

Substituting (70) into (19) and referring to (68) and (69) yields:

$$\begin{aligned} G_i\ddot{q}_i + \left\{\frac{1}{2}\dot{G}_i + S_i\right\}\dot{q}_i + c_i\dot{q}_i + \Delta f_i\{J_i^{\mathrm{T}}\bar{\mathbf{n}}_{0i} - (-1)^i(\mathbf{b}_i^{\mathrm{T}}\gamma_i)\mathbf{e}_i\} \\ + \Delta\lambda_i\{J_i^{\mathrm{T}}\bar{\mathbf{b}}_{0i} - (-1)^i(\mathbf{n}_i^{\mathrm{T}}\gamma_i)\mathbf{e}_i\} + \Delta N_i\mathbf{e}_i = 0, \quad i = 1, 2, \end{aligned} \tag{71}$$

where:

$$\Delta N_i = \beta\{(-1)^i l(\mathbf{b}_i^{\mathrm{T}}\gamma_i) - d(\mathbf{n}_i^{\mathrm{T}}\gamma_i)\} + \alpha_i\{p_i - p_i(0)\}, \quad i = 1, 2. \tag{72}$$

On the other hand, (1) and (2) can be rewritten into the forms:

$$M\ddot{\mathbf{x}} - \Delta f_1\bar{\mathbf{n}}_{01} - \Delta f_2\bar{\mathbf{n}}_{02} - \Delta\lambda_1\bar{\mathbf{b}}_{01} - \Delta\lambda_2\bar{\mathbf{b}}_{02} = 0 \tag{73}$$

$$I\ddot{\theta} - \Delta f_1(\mathbf{b}_{01}^{\mathrm{T}}\gamma_{01}) + \Delta f_2(\mathbf{b}_{02}^{\mathrm{T}}\gamma_{02}) + \Delta\lambda_1(\mathbf{n}_{01}^{\mathrm{T}}\gamma_{01}) - \Delta\lambda_2(\mathbf{n}_{02}^{\mathrm{T}}\gamma_{02}) + S_N = 0, \tag{74}$$

where:

$$S_N = \beta l(\mathbf{b}_{01}^{\mathrm{T}}\gamma_{01} - \mathbf{b}_{02}^{\mathrm{T}}\gamma_{02}) - \beta d(\mathbf{n}_{01}^{\mathrm{T}}\gamma_{01} + \mathbf{n}_{02}^{\mathrm{T}}\gamma_{02}) = \beta\{(s_1 - s_2)l + l_{\mathrm{w}}d\}. \quad (75)$$

Now it is possible to show that the set of equations (73)–(75) together with (7) can be regarded as a set of Euler–Lagrange equations obtained by applying the variational principle to the Lagrangian:

$$L = K(X, \dot{X}) - U(s_1, s_2) + \sum_{i=1,2}(\Delta f_i Q_{ni} + \Delta\lambda_i Q_{bi}), \quad (76)$$

in which the external forces of damping $c_i\dot{q}_i$ for $i = 1, 2$ through finger joints are taken into account. In fact, from (27)–(29) and (A.1) in Appendix A it follows that:

$$\frac{\mathrm{d}U(s_1, s_2)}{\mathrm{d}t} = \sum_{i=1,2}\frac{\mathrm{d}U_i}{\mathrm{d}s_i}\frac{\mathrm{d}s_i}{\mathrm{d}t} = \sum_{i=1,2}(-1)^i\beta\{(\mathbf{n}_i^{\mathrm{T}}\gamma_i)d - (-1)^i(\mathbf{b}_i^{\mathrm{T}}\gamma_i)l\}\kappa_i\frac{\mathrm{d}s_i}{\mathrm{d}t}$$

$$= \sum_{i=1,2}\beta\{(\mathbf{n}_i^{\mathrm{T}}\gamma_i)d - (-1)^i(\mathbf{b}_i^{\mathrm{T}}\gamma_i)l\}(\dot{\theta} - \dot{p}_i) \quad (77)$$

$$= \beta\{(\mathbf{n}_1^{\mathrm{T}}\gamma_1 + \mathbf{n}_2^{\mathrm{T}}\gamma_2)d + (\mathbf{b}_1^{\mathrm{T}}\gamma_1 - \mathbf{b}_2^{\mathrm{T}}\gamma_2)l\}\dot{\theta} + \sum_{i=1,2}\beta N_i\dot{p}_i, \quad (78)$$

where N_i is defined as:

$$N_i = (-1)^i(\mathbf{b}_i^{\mathrm{T}}\gamma_i)l - (\mathbf{n}_i^{\mathrm{T}}\gamma_i)d. \quad (79)$$

By using (28) and (29), (78) can be written as:

$$\frac{\mathrm{d}U(s_1, s_2)}{\mathrm{d}t} = \beta\{(l + l_{\mathrm{w}})d + (s_1 - s_2 - d)l\}\dot{\theta} + \sum_{i=1,2}\beta N_i\dot{p}_i$$

$$= S_N\dot{\theta} + \sum_{i=1,2}\beta N_i\mathbf{e}_i^{\mathrm{T}}\dot{q}_i. \quad (80)$$

Thus, we conclude that from (72) the variation of P takes the form:

$$\mathrm{d}P = d\left[U + \sum\frac{\alpha_i}{2}\{p_i - p_i(0)\}^2\right]$$

$$= S_N\mathrm{d}\theta + \sum_{i=1,2}[\beta N_i + \alpha_i\{p_i - p_i(0)\}]\,\mathrm{d}p_i$$

$$= S_N\mathrm{d}\theta + \sum_{i=1,2}\Delta N_i\mathbf{e}_i^{\mathrm{T}}\,\mathrm{d}q_i. \quad (81)$$

The last term of the left-hand side of (74) comes directly from the first term of the right-hand side of (81) in the variational form of the potential $P(X, s_1, s_2)$. The last term $\Delta N_i\mathbf{e}_i$ also comes directly from the last term of (81). Thus, it is possible to prove that, if the posture of the fingers–object system satisfying the condition that $\overline{O_1O_2}$ is parallel to $\overline{P_1P_2}$ as shown in Fig. 3 is an isolated equilibrium state, then the posture must be asymptotically stable because the system is fully dissipated [9],

no matter how the system is holonomically constrained. If both the fingers are of 1 d.o.f., then the total degrees of freedom of the system becomes single and therefore the equilibrium state is isolated. In the case of a redundant degrees-of-freedom system like the setup illustrated in Fig. 1, it is necessary to extend the so-called Dirichlet–Lagrange stability theorem [9, 10] to a system with redundancy in degree of freedom together with holonomic constraints. Such an extension of the theorem is possible as already discussed in a special class of robot control problems [11], but the details are too mathematically sophisticated and therefore will be discussed in a future paper.

7. Conclusions

Characterization of a desired fingertip geometry of a robot hand for precision prehension of 2-D objects with arbitrary shapes is discussed on the basis of Euler–Lagrange equations of motion of physical interactions between fingertip contour curves and object surfaces. Based on the use of control signals from the fingers–thumb opposability, a region of the desired fingertip contour is characterized by its curvature relative to the distance from the fingertip center to the tangent at the contact point. From the stabilization point of view of grasping, it is shown that a typical human thumb has a wider region in the contour curve than other fingertip geometries, such as an ellipse or a crescent moon type.

References

1. J. Napier, *Hands*. Princeton University Press, Princeton, NJ (1993).
2. S. Arimoto, Intelligent control of multi-fingered hands, *Annu. Rev. Control* **28**, 75–85 (2004).
3. S. Arimoto, *Control Theory of Multi-fingered Hands: A Modelling and Analytical-Mechanics Approach for Dexterity and Intelligence*. Springer, London (2008).
4. R. Murray, Z. Li and S. S. Sastry, *A Mathematical Introduction to Robotic Manipulation*. CRC Press, Boca Raton, FL (1994).
5. S. Arimoto, M. Yoshida, M. Sekimoto and K. Tahara, Modeling and control of 2-D grasping of an object with arbitrary shape under rolling contact, *SICE J. Control Meas. Syst. Integrat.* **2**, 379–386 (2009).
6. K. Nomizu, Kinematics and differential geometry of submanifolds — rolling a ball with a prescribed locus of contact, *Tohoku Math. J.* **30**, 623–637 (1978).
7. S. Arimoto, M. Yoshida, M. Sekimoto, K. Tahara and J.-H. Bae, Modeling and control for 2-D grasping of an object with arbitrary shape under rolling contact, in: *Proc. SYROCO 2009*, Gifu, pp. 517–522 (2009).
8. S. Arimoto, A differential-geometric approach for 2D and 3D object grasping and manipulation, *Annu. Rev. Control* **31**, 189–209 (2007).
9. W. M. Oliva, *Geometric Mechanics (Lecture Notes in Mathematics 1798)*. Springer, Berlin (2002).
10. F. Bullo and A. D. Lewis, *Geometric Control of Mechanical Systems*. Springer, New York (2005).
11. S. Arimoto, M. Sekimoto, H. Hashiguchi and R. Ozawa, Natural resolution of ill-posedness of inverse kinematics for redundant robots: a challenge to Bernstein's degrees-of-freedom problem, *Adv. Robotics* **19**, 401–434 (2005).

Appendix A

Partial differentiation of $U(s_1, s_2)$ of (27) in s_i results in:

$$\begin{aligned}\frac{\partial U}{\partial s_i} &= \beta\left\{d\frac{\partial d}{\partial s_i} + l\frac{\partial l}{\partial s_i}\right\} \\ &= (-1)^i\beta\kappa_i\{(\mathbf{n}_i^{\mathrm{T}}\gamma_i)d - (-1)^i(\mathbf{b}_i^{\mathrm{T}}\gamma_i)l\} \\ &= (-1)^i\beta\kappa_i(\mathbf{r}_1 - \mathbf{r}_2)^{\mathrm{T}}\bar{\boldsymbol{\xi}}_i, \quad i = 1, 2. \end{aligned} \tag{A.1}$$

Further, since $\bar{\mathbf{n}}_{0i}$ and $\bar{\mathbf{b}}_{0i}$ are irrelevant to s_i and $(\mathbf{r}_1 - \mathbf{r}_2)^{\mathrm{T}}\mathbf{b}_{0i} = 0$ at $s_i = s^*$, it follows that $(\mathbf{r}_1 - \mathbf{r}_2)^{\mathrm{T}}\partial\bar{\boldsymbol{\xi}}_i/\partial s_i = l(s_1, s_2)\partial(\mathbf{b}_i^{\mathrm{T}}\gamma_i)/\partial s_i$ at $s_i = s^*$ and:

$$\begin{aligned}\left.\frac{\partial^2 U}{\partial s_i^2}\right|_{s_i=s^*} &= -\beta\kappa_i(\mathbf{r}_1 - \mathbf{r}_2)^{\mathrm{T}}\left.\frac{\partial\bar{\boldsymbol{\xi}}_i}{\partial s_i}\right|_{s_i=s^*} \\ &= -\beta\kappa_i l(\mathbf{b}_i^{\mathrm{T}}\gamma_i' + \kappa_i\mathbf{n}_i^{\mathrm{T}}\gamma_i) \\ &= -\beta\kappa_i^2 l(1/\kappa_i + \mathbf{n}_i^{\mathrm{T}}\gamma_i), \end{aligned} \tag{A.2}$$

which shows (39).

Appendix B

From the definition of N_1 in (52) and the derivative of $U(s)$ in s as shown in (58), it follows that:

$$\frac{\mathrm{d}U}{\mathrm{d}t} = \frac{\mathrm{d}U}{\mathrm{d}s}\frac{\mathrm{d}s}{\mathrm{d}t} = \beta(\kappa_0 + \kappa_1)N_1\frac{\mathrm{d}s}{\mathrm{d}t}. \tag{B.1}$$

Substitution of (55) into the right-hand side of (B.1) yields:

$$\frac{\mathrm{d}U}{\mathrm{d}t} = \beta(\dot{\theta} - \mathbf{e}^{\mathrm{T}}\dot{q})N_1, \tag{B.2}$$

which shows:

$$\mathrm{d}U(s) = -\beta N_1\mathrm{d}\theta + \beta N_1\mathbf{e}^{\mathrm{T}}\mathrm{d}q. \tag{B.3}$$

The last term in the left-hand side of (53) comes from the first term of the right-hand side of (B.3) and the last term in the right-hand side of (54) comes from the second term of that of (B.3).

About the Authors

Suguru Arimoto received the BS from Kyoto University, in 1959, and DE from the University of Tokyo, in 1967. He was an Associate Professor of Osaka University during 1968–1973, and a Professor, during 1973–1990. In 1988, he joined the Faculty of Engineering of the University of Tokyo as a Professor and, in 1997, retired. Since 1997, he has been with Ritsumeikan University as a Professor. He is an IEEE Fellow (1983), an IEICE Fellow (2000), an RSJ Fellow (2003), a JSME Fellow (2005) and an IEEE Life Fellow (2007). He was awarded a Royal Medal with a Purple Ribbon from the Japanese Government in 2000, IEEE 3rd Millennium Memorial Medal in 2000, Pioneer Award from the IEEE R&A Society in 2006, and the 2007 Rufus Oldenburger Medal from the ASME.

Morio Yoshida received the BS, MS and DE degrees from Ritsumeikan University, Japan, in 2002, 2004 and 2007, respectively. He is currently a Research Scientist in RIKEN-TRI Collaboration Center, RIKEN, Japan. His current research interests are robot hands, modeling and robot control.

Masahiro Sekimoto received the BS, MS and PhD degrees from Ritsumeikan University, Japan, in 2003, 2005 and 2007, respectively. In 2007, he joined the Research Organization of Science and Engineering of Ritsumeikan University, where he is currently a Postdoctoral Fellow. He was a Visiting Scholar at Georgia Institute of Technology, USA, in 2008. His research interests include control design of redundant robots and mechanical analyses of human movements.

Ji-Hun Bae received the BS and MS degrees in Electrical Engineering from Myongji University, South Korea, in 1999 and 2001, respectively, and the PhD degree in Robotics from Ritsumeikan University, Japan, in 2004. He is currently a Research Scientist at DART (Division for Applied Robot Technology), KITECH (Korea Institute of Industrial Technology). From 2004 to 2006, he was a Postdoctoral Fellow at the 21st Century COE Program at Ritsumeikan University, Japan. He worked as a Senior Researcher at PIRO, from 2006 to 2008, and as a Postdoctoral Fellow at KIST, from 2008 to 2009. His research interests include robot manipulation, robot hands and arms, sensory feedback control, biological control and bio-mimetics.